The contribution of paleomagnetism, tephro-chronology, and radiocarbon dating to refine the last 1100 years of eruptive activity at Vulcano (Italy)

Arianna Beatrice Malaguti[1,2,3], Mauro Rosi[2], Marco Pistolesi[2], Fabio Speranza[3] & Martin Menzies[4]

[1]Dipartimento di Scienze Pure e Applicate, Università degli studi di Urbino Carlo Bo, Via Ca' le Suore 2/4, 61029 Urbino, Italy

[2]Dipartimento di Scienze della Terra, Università di Pisa, Via S. Maria 53, 56126 Pisa, Italy

[3]Istituto Nazionale di Geofisica e Vulcanologia, Sezione di Roma 2, Via di Vigna Murata 605, 00143 Roma, Italy

[4]Department of Earth Sciences, Royal Holloway University of London, Egham, Surrey, TW20 OEX England

ABSTRACT

During the past millennia, several eruptions have occurred within the La Fossa caldera on the island of Vulcano (Aeolian Islands, Italy), some being also described in historical documents dating back to Republican Roman times (I-II century BC). The absolute and relative timing of such activity, however, has remained poorly defined and controversial, due to contrasting ages provided by radiometric and unconventional paleomagnetic methods. Here we present a detailed reconstruction of the eruptive history focused on the IX - XV century AD period, that occurred at both La Fossa cone and Vulcanello. This integrated approach involves tephrostratigraphy, standard paleomagnetic methodology and radiocarbon dating. The new dataset confirms that the lavas exposed above sea level at Vulcanello were erupted between the X and XI century AD, and not between the I and II century BC as previously suggested. In this same time interval, La Fossa cone was characterized by long-lasting, shoshonitic, explosive activity followed by a discrete, sustained, rhyolitic explosive eruption. Between AD 1050 and 1300, activity was focused only on La Fossa cone, with alternating explosive and effusive eruptions that emplaced four rhyolitic and trachytic lava flows, resulting in significant growth of the cone. After the violent, phreatic event of the Breccia di Commenda (XIII century), the eruption continued with a substantial, long-lasting emission of fine ash until activity ceased. Magmatic explosive activity resumed at La Fossa cone at the beginning of the XV century marking the onset of the Gran Cratere cycle. This phase lasted until the mid-XVI century and produced at least seven explosive eruptions of intermediate magma composition and a couple of lateral explosions (Forgia Vecchia I and II). During this time interval, a third cinder cone was emplaced at Vulcanello, and the activity produced the lava flows of Punta del Roveto and Valle dei Mostri. From the XVII to XX centuries, volcanic activity was concentrated at La Fossa cone, where it ended in 1890.

This work confirms that Vulcanello island formed in Medieval times between the X and XI centuries. Moreover, between the X and mid-XVI centuries, La Fossa caldera was the site of at least 19 eruptions with an average eruption rate of one event every 34 years. This rate makes volcanic hazard at Vulcano higher than that suggested to date.

Keywords: tephro-stratigraphy, paleomagnetic dating, radiocarbon, Vulcano island, Vulcanello

INTRODUCTION

A detailed knowledge of the timing and characteristics of the eruptive history of active volcanoes is pivotal in evaluating volcanic hazards and unravelling volcanic/magmatic systems.

Reconstructions of past activity have been compiled at different well-known active volcanoes worldwide based on tephro-stratigraphic and physical volcanological studies, coupled with a large number of radiometric dates (Mt. St. Helens in USA, Pallister et al. 2017; Vesuvius in Italy, Cioni et al. 2008; Cotopaxi in Ecuador, Pistolesi et al. 2011; Izu-Oshima in Japan, Yamamoto 2017). Accurate investigations of volcanic history and assessment of eruptive parameters have provided the background for model-based hazard assessments of tephra fallout, vent opening and pyroclastic density flows at Vesuvius and Phlegrean Fields in Italy (Macedonio et al. 2008; Bevilacqua et al. 2015; Neri et al. 2015). These result in comprehensive volcano-magmatic models of volcanic systems (Santorini (Greece), Andujar et al. 2016; Mt. St. Helens (USA), Pallister et al. 2107; Vesuvius (Italy), Scaillet et al. 2008).

Fieldwork-based reconstructions of volcanic histories is more complicated at volcanoes characterized by explosive events of moderate intensity and magnitude, where tephra deposits mostly consist of very similar fine-grained, ash layers. In addition, ash deposits are easily eroded resulting in poor preservation in the stratigraphic record. The volcanic system of Vulcano (Vulcano Island, Southern Italy), is one of the iconic global volcanoes whose last eruption in 1888-90 offered G. Mercalli the chance to outline the characteristics of what would become the most famous explosive styles worldwide (i.e., the “Vulcanian” eruptive style; Mercalli and Silvestri 1891). The way in which the activity of Vulcano unfolds consists of the long-lasting repetition of impulsive, short-lived individual Vulcanian bursts and the launch of ballistic blocks and bombs along with the formation of ash-laden convective plumes that rise for a few km. Ash and lapilli fallout generates stratified, similar ash and lapilli tephra layers within a few km of the vent. Over the past decades, a wealth of studies addressed the geological mapping of the entire island and the recognition of the main eruptive units (De Astis et al. 2013; Selva et al. 2020). However, tephrostratigraphy of the most recent activity lacked accurate data. In addition, past investigations have been for long time based studies on a limited number of radiometric dating. To date, the only radiometric ages consist of a few K/Ar (Frazzetta et al. 1984) and ^{266}Ra/^{230}Th age determinations (Voltaggio et al. 1995; Soligo et al. 2000), that are unsuitable for establishing the age of units erupted in the last thousand years.

In the last decades, publication of paleomagnetic ages on lavas and high temperature pyroclastic flow deposits (Arrighi et al. 2006; Zanella 2006; Gurioli et al. 2012) provided new significant data. The inadequate number and typology of chronological data and the lack of a comprehensive tephrostratigraphic analysis suitable to tackle the high number of ash units, was the principal motivation in undertaking the present study.

The methodology was targeted to resolve the volcanic history of the period between the IX and XV centuries. It consisted of a significant number of conventional paleomagnetic dates of lava flows, welded scoriae and a dyke combined with a tephro-stratigraphic analysis and ^{14}C ages dating of some relevant tephra units. Tephrostratigraphic and geochronological reconstructions strongly benefitted from new data and charcoal samples collected from machine excavated trenches. This tephrostratigraphic survey also gained from the recent work of Pistolesi et al. (2021) who identified and dated exotic rhyolite ash beds on Lipari that were correlated and traced across different sectors of the island.

Our work was able to recognize and date a large number of events at La Fossa caldera, enabling us to uncover rapid variations in eruption style and magma composition at la Fossa, and also to reveal the quasi-synchronous pattern of activity between eruptive vents situated a few km apart within the same caldera system.

CHRONOSTRATIGRAPHIC FRAMEWORK

Vulcano is the southernmost island of the Aeolian volcanic arc, located in the Southern Tyrrhenian Sea (Fig. 1). According to De Astis et al. (2013), it formed during eight eruptive epochs, from

~130 ka to the present day. The most recent activity of La Fossa cone and Vulcanello has been the target of several studies that have proposed different reconstructions (Keller 1980; De Astis et al. 2013; Di Traglia et al. 2013; Fusillo et al. 2015; Selva et al. 2020). Using radiometric ages, the stratigraphic succession of La Fossa cone was divided into three major sequences (De Astis et al. 2013). The lower part includes the Punte Nere and Grotta di Palizzi 1 formations, erupted between BC ~3550 and 950 (Table 1; Frazzetta et al. 1984; Voltaggio et al. 1995; Soligo et al. 2000). The intermediate portion (Grotta di Palizzi 2 and 3, Carruggi and Forgia Vecchia formations) was emplaced between BC ~250 to AD 776 (Table 1; Keller 1980; Frazzetta et al. 1984). The upper sequence is characterized by the Pietre Cotte and Gran Cratere formations erupted between AD 1739 and AD 1890-1890 (Mercalli and Silvestri 1891).

Di Traglia et al. (2013) proposed a different reconstruction relying on tephro-stratigraphic and geomorphological considerations (Fig. 1). According to Di Traglia et al. (2013), the most recent part of the La Fossa cone sequence can be divided in two eruptive clusters (i.e., Palizzi-Commenda and Gran Cratere). The Palizzi-Commenda eruptive cluster encompasses the Grotta di Palizzi 2 and 3 of De Astis et al. (2013). The significant difference with respect to the stratigraphy proposed by De Astis et al. (2013) also concerns the Punte Nere lava flow (which De Astis et al. 2013 considered at BC ~3550) that was included in the Palizzi sequence based on the paleomagnetic age (AD 1170) proposed by Arrighi et al. (2006). According to Di Traglia et al. (2013), three trachytic lava flows were erupted at the end of Palizzi tephra unit: Punte Nere, Campo Sportivo and Palizzi (AD 1230±20; Arrighi et al. 2006). The trachytic lavas were followed by the emplacement of the rhyolitic Commenda lava (AD 1250±100; Arrighi et al. 2006). The activity then resumed with a violent hydrothermal explosion, the age and the origin of which is still debated: the Breccia di Commenda (XIII century) of Gurioli et al. (2012) and Rosi et al. (2018), or Carruggi formation (VIII century) of De Astis et al. (2013). After a period of eruptive quiescence, the activity at La Fossa cone resumed with the Gran Cratere Eruptive cluster, that encompasses the lateral hydrothermal explosions of Forgia Vecchia I (AD 1444; Mercalli and

Silvestri 1891) and the Forgia Vecchia II (AD 1727; Di Traglia et al. 2013; Selva et al. 2020), the Pietre Cotte lava flow (AD 1739; Arrighi et al. 2006) and ends with the AD 1888-1890 eruption (Mercalli and Silvestri 1891).

As a whole, De Astis et al. (2013) reported the onset of Punte Nere and Palizzi activity at BC 3550 and 950 respectively, whereas Di Traglia et al. (2013) and Fusillo et al. (2015) suggested a younger age (AD 1170 and 1230, respectively) on the basis of tephro-stratigraphic evidence and archaeomagnetic results (Arrighi et al. 2006).

The controversial age of Vulcanello

The activity of Vulcanello is commonly divided into three lithosomes (Vulcanello I, II and III), with each of them associated with explosive activity eventually producing three partially overlapping pyroclastic cones (Cone I, II and III), a basal lava platform and multiple lava flows (De Astis et al. 2013; Fusillo et al. 2015; Fig. 1). The temporal evolution of Vulcanello is controversial. According to Keller (1970, 1980), the early eruptions were dated to BC 126 or 183, on the basis of historical chronicles provided by Strabo and Plinius, quoted by De Fiore (1922) and Mercalli and Silvestri (1891), and based on ^{266}Ra/^{230}Th radiometric data (Voltaggio et al. 1995). The Republican Roman age (BC I-II century) of the Vulcanello lava platform was believed to be confirmed by the presence of an exotic rhyolitic ash layer on top of the lava, attributed to the AD 776 Mt. Pilato eruption from nearby Lipari (Keller 1980; De Astis et al. 2013).

Conversely, paleomagnetic data (Arrighi et al. 2006) led to the proposal that Cone I and its lava flows were erupted around AD 1000-1100, and that the whole lava platform developed in different stages between AD 1100 and 1250. This latter hypothesis was also accepted by Davì et al. (2009), Gurioli et al. (2012), Di Traglia et al. (2013) and Pistolesi et al. (2021), who proposed that the white rhyolite tephra overlying the Vulcanello lava platform belongs to the younger Rocche Rosse eruption from Lipari (AD 1243-1304; Pistolesi et al. 2021).

An erosive unconformity separates the volcanic products of Vulcanello I from those of Vulcanello II (De Astis et al. 2013; Fusillo et al. 2015). The explosive activity of Vulcanello cone II renewed with the emplacement of a submarine pillow lava field located offshore NE Vulcanello (Gamberi et al. 1997; Gamberi 2001; Romagnoli et al. 2013). The lava field was most likely fed by a dike exposed on the northern cliff of Cone I (Fusillo et al. 2015). The Vulcanello I and II deposits are blanketed by tephra deposits from both La Fossa cone (Palizzi rhyolitic lapilli and ash deposits from the Breccia di Commenda eruption) and Lipari (the rhyolite tephra described above and attributed to Mt. Pilato activity by De Astis et al. (2013) and to Rocche Rosse by Di Traglia et al. (2013), Fusillo et al. (2015) and finally dated by Pistolesi et al. (2021)). The initial part of Vulcanello III consists of black tephra deposits and the Punta Roveto and Valle dei Mostri lava flows (Fusillo et al. 2015). Organic matter found in a paleosol formed during a period of dormancy during these phases and dated by ^{14}C at BP 0.397±0.097 ka (Keller 1970), further constrains the last part of Vulcanello III activity, that resumed with the deposition of final tephra units.

METHODS AND WORK STRATEGY

To carry out an accurate revision of the La Fossa cone-Vulcanello tephrostratigraphy and chronology over the past 1100 years, we have employed three complementary methods: i) tephro-stratigraphy involving digging of trenches in suitable sites at La Fossa cone and Vulcanello; ii) ^{14}C dating of five charcoal fragments recovered from the trenches; and iii) paleomagnetic dating of eight different eruptive units sampled at fifteen sites (i.e., 174 oriented cores). An important contribution to the tephra stratigraphy was provided by the dig of ~20, two to three m-deep, trenches at increasing distances from the La Fossa cone in flat sites considered suitable for recording primary sequences and with high preservation potential (Fig. 2d). Some of the trenches were located in areas of particular stratigraphic interest being placed between La Fossa cone and Vulcanello islet. Tephra logging was done at each site; thanks to preservation of deposits across multiple places, precise correlations among tephra units outcropping at different sites were possible and based on their sedimentological characteristics (grain-size, colour, thickness, stratification and gradation, componentry and dispersal). Lava bodies and tephra beds emplaced during the effusive phases were identified and assigned based on stratigraphic correlations (Fig. 2a, b).

In addition, to help in elucidating the tephra stratigraphy, the trenches had the invaluable merit to allow the recovering of charcoal remnants at different stratigraphic levels. ^{14}C dates were performed by the Oxford Radiocarbon Accelerator Unit (ORAU). All the samples underwent pre-treatment processes with HCl (10% conc.) in order to remove any absorbed carbonates and then measured using an Accelerator Mass Spectrometer (AMS). The charcoals were chemically pre-treated using the acid-base-acid (ABA) methodology outlined by Brock et al. (2010). The radiocarbon ages were calibrated in OxCal v4.4 (Ramsey et al. 2009) using the IntCal20 calibration curve (Reimer et al. 2020) and are presented in calendar years AD.

During June 2018 and May 2019, 174 oriented paleomagnetic cores were collected from 15 sites belonging to 8 units (lava and welded scoriae) from both La Fossa cone and Vulcanello (Table S1; Fig. 1). We sampled two lavas and welded scoriae from the Palizzi-Commenda eruptive cluster, and the whole sequence of Vulcanello effusive products with the exception of the lava platform. The Punte Nere unit of Keller (1980) and De Astis et al. (2013) incorporates both the spatter bed exposed in the marine cliff south of Porto Levante Bay (previously investigated by Arrighi et al. 2006), and also the lava fan that formed the Punte Nere Cape (already sampled by Lanza and Zanella 2003). However, because the stratigraphic relationships between the two deposits are not clear (see below), in this work we decided to sample and treat both units at the five different sites separately.

For the paleomagnetic work we followed the classic sampling methods, laboratory instruments, procedures and statistical treatments already described by Speranza et al. (2008). Details on paleomagnetic methods are provided in the supplementary section.

Palaeomagnetic dating was carried out using the Matlab tool of Pavón-Carrasco et al. (2011). The volcanic unit-mean paleomagnetic directions (average of characteristic remanent magnetization directions (ChRMs) from all sites belonging to the same volcanic unit) were compared with the SCHA.DIF.4K paleo-secular variation (PSV) regional model (covering the last 4 ka, Pavón-Carrasco et al. 2021), and -only for the likely older Punte Nere Spatter- with the SHA.DIF.14K PSV global model (covering the last 14 ka, Pavón-Carrasco et al. 2014). Input age windows relied on stratigraphy, radiometric (^{14}C, K/Ar, Ra^{266}/Th^{230}) constraints, and historical chronicles. Paleomagnetic data from lavas, scoriae and pyroclastic rocks of Vulcano were already reported by Lanza and Zanella (2003) who analysed the PSV of the Earth's magnetic field during the last 135 ka, and by Arrighi et al. (2006) and Zanella (2006) who dated using PSV analysis the most recent (last 2200 years) eruptions and were thus compared with our results.

RESULTS

Stratigraphy and ^{14}C datings

Fieldwork carried out at La Fossa cone and Vulcanello allowed us to further investigate the architecture of the tephra deposits previously outlined in Di Traglia et al. (2013) and Fusillo et al. (2015), and also to correlate stratigraphic relationships between the two eruptive centres. The deposits encompass a series of tephra units associated with Vulcanian activity (Palizzi and Gran Cratere), interlayered with tephra beds produced by higher intensity eruptive events (Fig. 2). Although the eruptive period after the Breccia di Commenda encompasses deposits including the Pietre Cotte lava flow and the 1888-90 eruption, we limited this study to the older portion, from the onset of the Gran Cratere activity to the Forgia Vecchia II explosion. Locations of trenches and of natural outcrops used for tephra correlations are reported in Figure 2d.

A selection of four trench logs from the south-eastern side of the La Fossa cone and from different sectors of the lava platform of Vulcanello is presented in Figure 3. The logs provide information in terms of relationships between the main tephra units, evidence of time breaks and the occurrence of tephra markers across La Fossa cone and Vulcanello. The largest and deepest trench

(13×5.7×5.2 m) was dug about 1 km SE from the AD 1888-90 crater of La Fossa cone, in the upper segment of the Palizzi Valley (Fig. 3d). The trench crossed about 3.7 m of almost fully parallel, base to top, tephra deposits (the succession of Palizzi of Di Traglia et al. 2013). The sequence is bounded at the base by slightly altered, massive dark ash embedding charcoal fragments (samples CHP1 and CHP2), and at the top by the Rocche Rosse/Breccia di Commenda deposits (Figs. 2a, 3d). From the base, PalA, PalB and PalC consist of primary, plane-parallel, dark-coloured ash and lapilli fallout deposits with no interposition of reworked material, suggesting that the entire sequence was erupted in a fairly short time interval. PalA is a 50 cm-thick, stratified, dark ash and lapilli-bearing sequence overlaid by 10 cm-thick, white-coloured rhyolitic ash and pumice lapilli fallout (PalB marker bed). PalB is in turn overlaid by a ~2 m-thick, thinly stratified, dark-coloured ash and lapilli fallout deposits (PalC) and higher up by another 60-70 cm of reworked deposits indicating the presence of a hiatus before the deposition of PalD. In another trench located a few hundred meters north (Fig. 2a), a 70 cm-thick tephra sequence consisting of plane-parallel, thinly stratified ashes separates the PalD and Rocche Rosse/Breccia di Commenda units. The lowermost 10 cm consist of light grey to white fine ash that we correlate with a tephra deposit emplaced during the effusive activity of Commenda lava. In contrast, the overlying dark grey-coloured stratified ash deposits are correlated with the Campo Sportivo and Palizzi lava flows, suggesting that they were erupted before (or in connection with) effusive activity. Another trench (Fig. 2b) about two m deep, located ESE of le Fossa cone in a natural cut exposed in a gully about 100 m east of the Palizzi lava flow, was also crucial and confirmed the presence of tephra deposits between the pumice bed PalD and the Rocche Rosse and Breccia di Commenda units. The trench reveals the presence of 60 cm-thick, thinly stratified, light grey, fine ash that suggests the existence of mild explosive activity pene-contemporaneous to the Commenda, Punte Nere, Campo Sportivo and Palizzi lava flows. The identification of this ash units above PalD definitely corroborates that the rhyolitic pumice eruption (PalB) and the Commenda rhyolite lava flow were not erupted in sequence, but rather that Commenda lava was emplaced after PalD and before Campo Sportivo and Palizzi lavas.

The three trenches dug on Vulcanello encompass the entire tephra sequence accumulated onto the Vulcanello structure. The rhyolite pumice fallout (PalB marker bed) erupted at La Fossa cone, ubiquitously overlies the lava platform with almost no interposition of other tephra (log (b) in Figure 3). Only in log (a) (Fig. 3), next to the base of the Vulcanello I and II cones, PalB overlies about 60 cm of tephra from the two cones, indicating that PalB was deposited after the formation of Cone II. Although some slight reworked deposits are interposed between the Vulcanello II tephra and PalB, field evidence indicate that Vulcanello I and II activity (and also the formation of the lava platform) shortly preceded the eruption of the rhyolite pumice at La Fossa cone (PalB).

The Rocche Rosse white rhyolitic tephra and the interfingered red to brownish varicolored ash of the Breccia di Commenda event represent traceable marker beds at La Fossa caldera and are also clearly present at Vulcanello in logs (b) and (c) (Fig. 3). At the top of the Breccia di Commenda ashes, reworked tephra and incipient weathering/soil formation indicates a significant hiatus (log (c) in Figure 3). The soil bed is in turn covered by coarse, grey coloured ashes of Vulcanello III, possibly preceded by the emplacement (in the Vulcanello area) of fine ash related to Forgia Vecchia I explosion from La Fossa cone (log (c) in Figure 3).

At La Fossa cone, an erosive unconformity marks the separation between the Breccia di Commenda final ashes, and the onset of the Gran Cratere activity (Fig. 2c). While the first Gran Cratere deposits are similar to the altered, post-Breccia di Commenda varicolored ashes, the following activity is characterized by fresh, stratified black to grey layers. Observations carried out within La Forgia Vecchia craters showed that the deposits filling the Forgia Vecchia I vent are represented by those coming from the Forgia Vecchia II younger explosion. Remarkably, those deposits alternate in the upper part and progressively migrate towards magmatic activity from La Fossa and showing similar characteristics of the onset of the Gran Cratere activity.

Five new radiocarbon dates were obtained from the charcoal fragments recovered from the trenches. Three out of five were recovered from Vulcanello (CS1, CS3 and CS6). Two (CHP1 and CHP2) were sampled from the trench dug in the upper segment of the Palizzi valley, the base of the Palizzi tephra sequence (Table 2).

The result of the charcoal CS1 collected from a hand dug pit 570 m NW of Vulcanello III crater yielded the uncalibrated date of 448±25 with a 95.4% chance of having an age between AD 1419 and 1470, which is equivalent to a calibrated age of BP 506±26. CS3 is a charcoal fragment collected from a trench dug 500 m south of the Vulcanello III crater. It shows an uncalibrated date of 461±26 and has a 95.4% chance of having an age between AD 1414 and 1458 (calibrated age of BP 514±22). Both charcoal fragments were recovered from the topmost part of the soil horizon underlying the Punta del Roveto tephra, thus providing an age close to the Punta del Roveto eruption. CS6 was collected from a hand dug pit 320 m N of Vulcanello III crater. The uncalibrated date of 717±22 has a 95.4% chance of having an age of between AD 1260 and 1298 (equivalent to a calibrated age of BP 671±19). The charcoal fragment was recovered from a 10 cm-thick reworked Commenda ash and the obtained age is to be considered correspondent to the Breccia di Commenda event.

The two charcoals from La Fossa caldera trench have remarkably similar ages. CHP1 has an uncalibrated date of 1084±24 corresponding to an age of between AD 895 and 1015 (calibrated age of BP 995±26), whereas CHP2 has an uncalibrated age of 1086±25, resulting in an age of between AD 896 and 1015 (or calibrated age of BP 995±61). The two ages result in a final calibrated age bracket of AD 895-1015, which can be confidently considered as the onset of the Palizzi sequence. This new age determination definitively confirms that the beginning of the Palizzi explosive activity occurred slightly before AD 1000.

Magnetic Properties

Representative outcrops used for paleomagnetic sampling are shown in Figure 4. The NRM values of the samples range between 0.1 and 44 A/m, although they mostly fall in the 1-10 A/m range (Fig. 5); magnetic susceptibilities are comprised between $4.6x10^{-2}$ and $3.5x10^{-4}$ SI (1.8 ± 0.15 $x10^{-2}$on average). The Königsberger ratio (Q) values of the samples are between 1 and 100 (Fig. S1a, b), confirming the predominance of remanent over induced magnetization also in more acidic and differentiated volcanics. Although – as a general rule – the different volcanic units fall in distinct diagram sectors, some units (e.g., Palizzi) show clustered magnetization values, while others (Punte Nere spatter) yield highly scattered values.

Thermomagnetic curves show the predominant occurrence of pure magnetite, with a Curie temperature (Tc) at ~580-600 °C, and an irreversible variation trend in the heating-cooling cycle (Fig. S2). In some specimens, an inflection on the heating curve around 400° C could indicate the occurrence of titanomagnetites and/or maghemite, whereas the cooling cycles show the unique occurrence of magnetite. In few samples, magnetic susceptibility values higher than zero at T>600 °C in the heating cycle suggest the additional presence of hematite, contributing subordinately to magnetic susceptibility.

The hysteresis properties (Fig. S3) reported on the Day-plot diagram (Dunlop 2002) show M_{rs}/M_s values comprised between 0.3 e 0.05 and B_{cr}/B_c values between 2.1 and 8.4. Samples are mainly clustered in the field of pseudo-single domain (PSD) magnetite field; most of them are aligned on the single-multi domain (SD-MD) mixing curve of the magnetite.

Paleomagnetic directions and dating

A well-defined ChRM was isolated for almost all samples in the 30-120 mT interval (Fig. 5). Site-mean declinations vary from 11.5° to 38.4°, while inclinations are comprised between 34.7° and 63.4° (Table 3; Fig. 6). The α_{95} values relative to the site-mean paleomagnetic directions vary from 2.7° to 7.0°, 4.9° on average. Sites VUL19 (Punte Nere spatter) and VUL27 (Commenda lava), whose α_{95} values are greater than 10°, were considered to be scattered (likely due to local block rotation/tilt) and discarded from further consideration.

Our paleomagnetic directions are consistent with those previously provided by Arrighi et al. (2006), and Lanza and Zanella (2003) for the same lava flows (Fig. 6), as the angular distances between our directions are those obtained by other authors from the same flows are generally <10°. Angular distance values ≤10° were in fact considered by many recent works as threshold for considering two sites belonging to the same volcanic unit at a 95% confidence limit (e.g., Pinton et al. 2018). Exception are the sites VN5 and VN13 sampled by Arrighi et al. (2006) in the Palizzi lava and Punte Nere Spatter (Figs. 1 and 6a) for which the difference - when compared to our sites VUL15 and VUL28 from the same units - is slightly higher (12.6° and 10.2°, respectively). We speculate that the slightly >10° angular distances observed between sites sampled by us and Arrighi et al. (2006) in the Palizzi lava and Punte Nere spatter might be due to the "blanket" demagnetization treatment used by Arrighi et al. (2006). In fact, such a laboratory procedure was abandoned in paleomagnetism since the 1970s (Van der Voo 1990), and has been shown to provide unrealistically small confidence cones (0.8°-1.8°) and age accuracies (20–30 years) in volcanics (e.g., Lanza et al. 2005; Speranza et al. 2006).

Palaeomagnetic dating (Table 3; Fig. 7) requires an input window age for the volcanics to be dated. For the Punte Nere welded scoriae, we considered a wide (BC 5000-AD 900) time interval, considering the whole geochronologic/paleomagnetic evidence (Frazzetta et al. 1984; Soligo et al. 2000; Casalbore et al. 2019), and we obtained a possible age of BC 3683-3541 (relying on the low probability density peak, we exclude the BC 932-901 and the AD 891-900 ages; Fig. 7 and Table 3). This age appears to be consistent with that of about 3550±1.3 ka BC found by Frazzetta et al. (1984) in case the radiometrically dated sample was taken from the spatter deposit mapped as part of the Punte Nere formation. In fact, the Punte Nere formation represents a complex series of deposits including a lava flow (forming the Punte Nere Cape; Figs. 1 and 4b), and variably welded spatter deposits cropping out at both sides of the lava (Fig. 4f). For the genuine Punte Nere lava flow, we used a time window between AD 900 to 1400 (the lava flow post-date the PalA tephra), obtaining an age of AD 1009-1168. For the Palizzi lava flow (Fig. 4e), we considered a BC 700 - AD 1500 age window, relying on K/Ar dating of Frazzetta et al. (1984), $^{266}Ra/^{230}Th$ age of Voltaggio et al. (1995), and paleomagnetic dating by Arrighi et al. (2006) and Zanella (2006), and we obtained an AD 1241-1305 paleomagnetic age.

With regards to Vulcanello I phase (Fig. 4a, d), we sampled the whole period of activity, including the lava forming the basal platform and the welded scoriae representing the final stages of Vulcanello I. A BC 200 - AD 1400 input time interval was thus considered, relying on historical chronicles, previous paleomagnetic dating, and $^{266}Ra/^{230}Th$ and ^{14}C constrains (De Fiore 1922; Mercalli and Silvestri 1891; Keller 1970; Voltaggio et al. 1995; Arrighi et al. 2006), and an AD 899-1044 paleomagnetic age was obtained (Fig. 7). For the dike feeding Cone II (Fig. 4a, c), we used an AD 700-1400 input age, considering stratigraphic constraints and ^{14}C ages (Keller 1970; Di Traglia et al. 2013; Fusillo et al. 2015; Rosi et al. 2018), and we obtained an AD 898-1022 time window (Fig. 7). Regarding the activity of Vulcanello III, we used an AD 1400-1800 input time interval for the first effusive activity (Punta del Roveto lava flow; Fig. 4g), based on ^{14}C dating obtained on charcoals underlying the Punta del Roveto tephra (see also Todman 2012). We obtained an AD 1400-1450 age (Fig. 7). Finally, for the last effusive phase of Vulcanello III (Valle dei Mostri lava; Fig. 4h), we considered the same input age window as for Punta Roveto, and we found an AD 1400-1466 paleomagnetic age (Fig. 7).

DISCUSSION

Chronostratigraphy of La Fossa Cone and Vulcanello

The integration of stratigraphic analysis, ^{14}C radiometric dating and paleomagnetism has allowed us to undertake high resolution timing of the last 1100 years of eruptive activity at La Fossa cone and Vulcanello. Herein we will discuss the new chronological framework of the different eruptive units, the chronostratigraphic relationships between La Fossa cone and Vulcanello and their significance for the caldera activity.

Punte Nere and Palizzi eruptive periods

The Punte Nere lava and spatter units represent a challenging topic in the recent volcanic history of La Fossa cone. The two units are mapped as a single formation in the geological map of Keller (1980), and also in the more recent map of De Astis et al. (2013), who used chronological constraints yielded by K/Ar (Frazzetta et al. 1984) and ^{266}Ra/^{230}Th (Soligo et al. 2000) data. However, Di Traglia et al. (2013) included the Punte Nere lava in the Palizzi eruptive cluster based on the paleomagnetic dating of Arrighi et al. (2006). Selva et al. (2020) have recently considered that such dual dating might reflect different sampling locations, since Casalbore et al. (2019) found (by a submarine geological survey) an underwater lava delta (Punte Nere old cycle) beneath the Punte Nere lava flow (recent cycle). Selva et al. (2020) suggest that Frazzetta et al. (1984) and Soligo et al. (2000) might have sampled the old cycle.

The lava delta forming the Punte Nere Cape is a multilobate, aa-type lava fan which extensively and continuously crops out from the shoreline (Fig. 1). Indeed, the very recent age (AD 1009-1168; Table 3; Fig. 7) of the aa lava accords well with the absence of any significant marine erosion (Romagnoli et al. 2013; Casalbore et al. 2019) and also by the presence, on top of the clinker bed, of the thin deposits belonging to the Breccia di Commenda sequence (Rosi et al. 2018). Conversely, the spatter unit (BC 3683-3541; Table 3; Figs. 2e, 7) exposed close to the coastline west of Punte Nere Cape is systematically truncated by marine erosion, and is covered by significant loose volcanic deposits and shows deep erosion. A further feature (that raises doubts on a common age for the spatter and the lava units) is the composition of the products that is trachytic for the lava of Punte Nere (Keller 1980) and latitic for the spatter deposit (Nicotra et al. 2018).

Our most probable age for the Palizzi lava flow is AD 1241-1305 (Table 3; Fig. 7), in agreement with paleomagnetic ages provided by Arrighi et al. (2006) and by Zanella (2006). The significantly younger ages provided by $^{266}Ra/^{230}Th$ (Voltaggio et al. 1995) are probably due to the instability of the isotope ^{226}Ra and by the complicated measurement procedure that can lead a wide range of errors (Voltaggio et al. 1995). Frazzetta et al. (1984) reported a K/Ar with a 2 kyr-long interval that encompasses all available ages. This inconsistency may derive from i) groundmass (instead of single crystal) K/Ar dating, because such procedure could have returned a significantly older dating than actual eruption age, and ii) possibly to the young age of the deposit which is unsuitable for K/Ar method. Indeed, it has been largely demonstrated that paleomagnetism is a more robust dating method than Ar/Ar or K/Ar for Holocene volcanic units (Arrighi et al. 2004; Speranza et al. 2008; Risica et al. 2019).

Vulcanello peninsula

The ages we provide for Vulcanello I (AD 899-1044; Table 3; Fig. 7) confirm that the subaerial portion of Vulcanello was emplaced during the Medieval Age, and not between the I and II centuries BC as suggested by De Fiore (1922), Mercalli and Silvestri (1891), Keller (1980), Voltaggio et al. (1995) and De Astis et al. (2013). This change to the onset of Cone I activity to the X century AD, indicates a similar age to the onset of the Palizzi activity at La Fossa cone (X century AD) and is in agreement with a recent review of historical sources (Manni and Rosi 2021). Despite the presence of a slight unconformity between the Cone I and Cone II deposits (Fig. 3a), the age for Cone II (from AD 898 to AD 1022; Table 3; Fig. 7) is statistically indistinguishable from Cone I, suggesting that the two cones were built in fairly rapid succession within ~150-200 years. The paleomagnetic age of the Punta del Roveto lava (AD 1400-1450; Table 3; Fig. 7) agrees with ^{14}C radiocarbon ages (AD 1420-1460) of charcoals immediately below the Punta del Roveto tephra (Table 2). Finally, the first paleomagnetic age obtained for the Valle dei Mostri lava flow (AD 1400-1466) turns out to be indistinguishable from that of the Punta del Roveto flow (Table

3; Fig. 7). This, coupled with the apparent absence of tephra interposed between Roveto and Valle dei Mostri lavas, may suggest that the two effusive units formed almost contemporaneously or in a close time interval (tens of years), before emplacement of the final tephra units of Vulcanello. This also agrees with the more recent age of 0.397±0.097 ka (AD 1553±97) obtained by Keller (1970). Keller (personal communication 2020) collected the charcoal from a soil horizon on the west side of the Cone III and thus above the Punta del Roveto lava. Consequently, this age represents an upper limit of the Punta del Roveto and Valle dei Mostri lavas, and a possible age for the tephra units Vulcanello 3C and 3D of Fusillo et al. (2015) which close the Vulcanello activity.

Timing of La Fossa and Vulcanello eruptions: implications for the caldera system behavior

Figure 8 summarises the overall chronological framework of the volcanic activity within La Fossa caldera in the time period AD 900-1600, highlighting the time-relationships between the activity at the two centres of La Fossa cone and Vulcanello. The reconstructed eruptive scheme is used to constrain the behaviour of the caldera system, given that La Fossa cone lies in the middle of the structure, while Vulcanello represents a peripheric apparatus placed at the caldera border (Casalbore et al. 2019).

The eruptive activity at La Fossa cone started with the emplacement of the Palizzi-Commenda Eruptive Cluster (PalA tephra unit) during mid-X century, 1000 years younger than that proposed by De Astis at al. (2013). This activity occurred penecontemporaneously with the onset of Vulcanello, where Cone I and the multi-flow lava platform were gradually built up, rapidly followed by the Cone II eruption (AD IX-X century). The deposits of the pyroclastic activity of La Fossa cone (PalB and PalC) lie directly above the Vulcanello lava platform and above Cone II deposits, with no interfingering of coarse, locally-derived tephra, suggesting that during PalB and PalC eruptions, activity at Vulcanello had ceased. Because we have never found in the trenches dug on the Vulcanello I lava platform any tephra belonging to PalA activity, we do conclude that:

i) the emplacement of the lava platform was immediately followed the explosive activity of PalB at La Fossa cone, and ii) PalA, Vulcanello I and II were penecontemporaneous and occurred within a short time interval. Deposit characteristics suggest that the whole activity at La Fossa cone during this first phase was explosive (from Vulcanian to subPlinian in style), while at Vulcanello effusive activity largely dominated over tephra emplacement and the explosive activity was accessory (small volume of the three cones) and dominated by mild strombolian activity (Fusillo et al. 2015). The sub-plinian style of PalB is suggested by the occurrence of pumice lapilli (2-3 cm in size) on Vulcanello coupled to deposit thickness up to 1 m west of La Fossa cone.

Volcanic activity temporary stopped at Vulcanello but continued at La Fossa cone (AD X-XII century). Although we have never observed stratigraphic relationships between PalC and Punte Nere lava, on the basis of our dating of the Punte Nere lava flow (AD 1009-1168), we suggest that PalC lies below the lava. After a period of quiescence, the PalD explosive eruption occurred, rapidly followed by the emplacement of the Commenda lava flow and tephra (AD 1250±100; Arrighi et al. 2006), Campo Sportivo and Palizzi lavas and tephra (AD 1241-1305; Fig. 8). Remarkably, this eruptive phase is characterized by effusive activity at La Fossa cone (with the exception of PalD and of thin ash deposits identified in the eastern sector of La Fossa cone), while Vulcanello shows no sign of activity. Stratigraphic relationships of tephras emplaced during rhyolitic and trachytic effusive activity suggest that the Commenda lava was emplaced after PalD tephra (at places the lava clearly overlies PalD tephra deposits) and slightly before Campo Sportivo and Palizzi lavas. The stratigraphic position of the Commenda lava between PalD and the Breccia di Commenda sequence is also confirmed by the occurrence of a grey to white ash bed in the tephra succession below the Breccia di Commenda deposits (Fig. 2a, b).

Between unconformities S2 and S3 (Fig. 8), the only explosive activity took place at La Fossa with the Breccia di Commenda Eruptive Unit, which is intercalated with the Rocche Rosse tephra from Lipari (Gurioli et al. 2012; Di Traglia et al. 2013; Rosi et al. 2018). The Rocche Rosse marker bed was dated at the end of XIII century (Pistolesi et al. 2021) and lie below the Vulcanello III initial tephra deposits, in agreement with their new radiocarbon age of early XIV century. The dynamics of the Breccia di Commenda has been extensively discussed by Gurioli et al. (2012) and Rosi et al. (2018). Gurioli et al. (2012) linked the large amount of lava lithics in the breccia to the lava clogging of the summit crater following the unusual effusive activity occurred at La Fossa cone between AD 1000 and 1200.

Later, after a period of stasis occurred at both La Fossa cone and Vulcanello activity (unconformity S3 of Di Traglia et al. (2013); log (c) in Figure 3), the volcanic activity resumed at La Fossa cone with the Gran Cratere Eruptive cluster (Fig. 8). Simultaneously, the volcanic activity at Vulcanello resumed with the emplacement of Vulcanello III tephra deposits (3A, 3B; Fusillo et al. 2015) and the Punta del Roveto and Valle dei Mostri lava (XIII century AD; Fig. 8). After a short rest, the activity at Vulcanello ended with the emplacement of final pyroclastic units (Vulcanello 3C, 3D; Fusillo et al. 2015), whose age is bracketed by the radiocarbon age of AD 1553±97 (Keller 1970; Fig. 8). At La Fossa cone, the activity continued from AD 1600 to 1890. During this phase started after S3, lateral phreatic explosions of Forgia Vecchia I and II occurred. While for the oldest, historical accounts indicate the 1444 as the most likely age, Forgia Vecchia II has been considered coincident with the 1727 event described in several chronicles (Selva et al. 2020). However, stratigraphic observations made within Forgia Vecchia craters may indicate an older age for the second event since its deposits are followed by the Gran Cratere activity, and which is possibly described in historical accounts during AD 1550.

Similarly to what we observed during the period AD 900-1100, activity at La Fossa cone after S3 showed explosive characteristics, while at Vulcanello effusive activity dominates over tephra. Alternation of effusive and explosive activity at the two centres suggests that La Fossa caldera had a behaviour such that when both centres were active, gas-rich magma was ejected at the main centre of La Fossa cone, with degassed magma feeding effusive activity deviated towards Vulcanello. In contrast, when Vulcanello showed no activity and La Fossa cone was active, both volatile-rich and volatile-poor magma rose sequentially in the main conduit. This conduit/feeding system connection has to be emplaced at some depth, given that shoshonitic and latitic magmas erupted at Vulcanello have an origin where a common feeding system with La Fossa cone may be present, while they migrated along a ring fault and last resided about 1 km beneath Vulcanello where they degassed before eruption (Fusillo et al. 2015). Remarkably, although the two post-caldera centres were fed by the same deep magmatic system (Davì et al. 2009; Fusillo et al. 2015), they showed contrasting eruptive behaviour in the last 1100 years of activity, with La Fossa cone producing mostly explosive eruptions, while at Vulcanello, degassed magma was generally emplaced as lavas.

CONCLUSIVE REMARKS

New paleomagnetic and radiocarbon dating, coupled to a detailed chrono-stratigraphic based on new stratigraphic data from dug trenches, successfully unravelled the timing of the eruptive activity at La Fossa caldera during the period 900-1600 AD:

- This work confirms that paleomagnetic dating, together with ^{14}C dating and stratigraphic surveys, allow a better resolution of the timing of Holocene volcanic products compared to other radiometric methods, and may be critical in unravelling the chronology of pre-historic volcanic eruptions.
- Our data confirms that Vulcanello island formed in Medieval times between AD 900 and 1050, and not between I and II centuries BC as previously suggested (Mercalli and Silvestri 1891; De Fiore 1922; Keller 1980; De Astis et al. 2013). We have shown that the formation of Cones I and II, the emplacement of the lava platform and of the pillow lava field offshore of Cone I were all pene-contemporaneous to an intense, purely explosive phase at La Fossa cone (eruption of PalA). Moreover, the activity of Vulcanello III was contemporaneous with the first part of the Gran Cratere cycle (AD 1420-1550). At La Fossa cone, this activity represents an important eruptive phase both in terms of magnitude and number of eruptive events.

- We propose a new interpretation for the Punte Nere unit, where we divide it into the Punte Nere old cycle (spatter unit; BC 3683-3541) and the Punte Nere recent cycle (lava flow; AD 1009-1168). In addition, we report higher resolution dates for the Palizzi lava flow and a possible stratigraphic position for the Commenda lava, which post-dates PalB-PalC and slightly predates Palizzi and Campo Sportivo lavas.
- Timing of the eruptive activity at La Fossa cone and Vulcanello clearly shows that when they are both active explosive activity is concentrated at La Fossa Cone, while effusive activity (lavas) is generally emplaced at Vulcanello. When only La Fossa conduit is active, the emission of degassed lava follows an initial phase of explosive activity. The occurrence of both explosive and effusive activity at La Fossa ultimately results in a more rapid growth of the cone.
- The new chronostratigraphic reconstruction provides a higher frequency of eruptions thus indicating a higher risk for La Fossa caldera. As reported by Selva et al. (2020), existing discrepancies among stratigraphic reconstructions for the eruptive successions of La Fossa cone and Vulcanello translate to variable mean recurrence rates in the reference period of the last 5 ka of activity. We emphasize that the younger ages of eruptions and the higher number of eruptive events results in a significantly increase in the frequency of the volcanic hazard, *with an average time recurrence of one event every 35 years between AD 850 and 1550, making the present repose time of almost 130 years as very unusual in the recent history of the volcano*. The occurrence of such clusters of intense volcanic activity before the eruption of 1888-90 underscores a very high risk for the La Fossa caldera which strongly contrasts with the widespread perception by Vulcano inhabitants of a low-risk volcano stemming from its, unusually long, state of quiescence. This is particularly crucial since, at the time of writing, the volcano current alert level has been raised from Green to Yellow in October 2021, due to increased seismicity, degassing and deformation of La Fossa cone (https://rischi.protezionecivile.gov.it/it/vulcanico/vulcani-italia/vulcano).

- We finally emphasize that several vents were active during the period AD 900-1600, both on Lipari and Vulcano islands, further strengthening the active role of a roughly NS-oriented, volcano-tectonic structure (Ventura et al. 1999; Gioncada et al. 2003; Ruch et al. 2016). Such rift in fact continues northward along the nearby Lipari Island, which was characterized by several quasi-contemporaneous eruptions during the XIV century AD (Gioncada et al. 2003; Forni et al. 2013; Ruch et al. 2016; Rosi et al. 2018; Pistolesi et al. 2021), suggesting the active role played by the fault system for the reactivation of the two volcanic islands.

Acknowledgements

G. Risica, I. Tubia, E. Billotta, E. Nicotra, R. De Rosa, P. Donato and M. Minniti are acknowledged for help and discussion in the field. The authors are grateful to C. Bonadonna (Univ. Geneve) for assistance during the fieldwork. We acknowledge G. De Astis for fruitful interactions on the geology of Vulcano. J. Keller is greatly thanked for providing information regarding the charcoal collected from a soil horizon on the west side of the Vulcanello Cone III. Comments by two anonymous referees and by the Associate Editor L. Pioli helped to significantly improve manuscript organization.

References

Andújar J, Scaillet B, Pichavant M, Druitt TH (2016) Generation conditions of dacite and rhyodacite via the crystallization of an andesitic magma. Implications for the plumbing system at Santorini (Greece) and the origin of tholeiitic or calc-alkaline differentiation trends in arc magmas. J Petrol, 57(10), 1887-1920

Arrighi S, Rosi M, Tanguy JC, Courtillot V (2004) Recent eruptive history of Stromboli (Aeolian Islands, Italy) determined from high-accuracy archeomagnetic dating. Geophys. Res. Lett. 31, L19603

Arrighi S, Tanguy JC, Rosi M (2006) Eruptions of the last 2200 years at Vulcano and Vulcanello (Aeolian Islands, Italy) dated by high-accuracy archeomagnetism. Phys Earth Planet Inter 159:225–233

Bevilacqua A, Isaia R, Neri A, Vitale S, Aspinall WP, Bisson M, Flandoli F, Baxter PJ, Bertagnini A, Esposti Ongaro T, Iannuzzi E, Pistolesi M, Rosi M (2015) Quantifying volcanic hazard at Campi Flegrei caldera (Italy) with uncertainty assessment: 1. Vent opening maps. J Geophys Res: Solid Earth 120(4), 2309-2329

Brock F, Higham T, Ditchfield P, Ramsey CB (2010) Current pretreatment methods for AMS radiocarbon dating at the Oxford Radiocarbon Accelerator Unit (ORAU). Radiocarbon 52(1):103-112

Casalbore D, Romagnoli C, Bosman A, De Astis G, Lucchi F, Tranne CA, Chiocci FL (2019) Multi-stage formation of La Fossa Caldera (Vulcano Island, Italy) from an integrated subaerial and submarine analysis. Mar Geophys Res. https://doi.org/10.1007/s11001-018-9358-3

Cioni R, Bertagnini A, Santacroce R, Andronico D (2008) Explosive activity and eruption scenarios at Somma-Vesuvius (Italy): towards a new classification scheme. J Volcanol Geotherm Res 178(3), 331-346

Davì M, De Rosa R, Donato P, Vetere F, Barca D, Cavallo A (2009) Magmatic evolution and plumbing system of ring-fault volcanism: the Vulcanello Peninsula (Aeolian Islands, Italy). Eur J Mineral 21:1009–1028

De Astis G, Lucchi F, Dellino P, La Volpe L, Tranne CA, Frezzotti ML, Peccerillo A (2013) Geology, volcanic history and petrology of Vulcano (central Aeolian archipelago). Geol Soc Lond Mem 37:281–349

De Fiore O (1922) Vulcano (Isole Eolie). Z Vulkanol 3:3–393

Di Traglia F, Pistolesi M, Rosi M, Bonadonna C, Fusillo R, Roverato M (2013) Growth and erosion: the volcanic geology and morphological evolution of La Fossa (Island of Vulcano, Southern Italy) in the last 1000 years. Geomorphology 194:94–107

Dunlop DJ (2002) Theory and application of the Day plot (M_{rs}/M_s versus H_{cr}/H_c): 1. Theoretical curves and tests using titanomagnetite data. J Geophys Res 107 (B3),2056. https://doi.org/10.1029/2001JB000486

Forni F, Lucchi F, Peccerillo A, Tranne CA, Rossi PL, Frezzotti ML (2013) Stratigraphy and geological evolution of the Lipari volcanic complex (central Aeolian archipelago). Geol Soc Lond Mem 37:213–279

Frazzetta G, La Volpe L, Sheridan MF (1983) Evolution of the Fossa cone, Vulcano. J Volcanol Geotherm Res 17:329–360

Frazzetta G, Gillot PY, La Volpe L, Sheridan MF (1984) Volcanic hazards of Fossa of Vulcano: data from the last 6,000 years. Bull Volcanol 47:105–124

Fusillo R, Di Traglia F, Gioncada A, Pistolesi M, Wallace PJ, Rosi M (2015) Deciphering post-caldera volcanism: insight into the Vulcanello (Island of Vulcano, Southern Italy) eruptive activity based on geological and petrological constraints. Bull Volcanol 77(9):76

Gamberi F (2001) Volcanic facies associations in a modern volcaniclastic apron (Lipari and Vulcano offshore, Aeolian Island Arc). Bull Volcanol 63(4):264–273

Gamberi F, Marani M, Savelli C (1997) Tectonic, volcanic and hydrothermal features of a submarine portion of the Aeolian arc (Tyrrhenian Sea). Mar Geol 140(1):167–181

Gioncada A, Mazzuoli R, Bisson M, Pareschi MT (2003) Petrology of volcanic products younger than 42 ka on the Lipari-Vulcano complex (Aeolian Islands, Italy): an example of volcanism controlled by tectonics. J Volcanol Geotherm Res 122-191–220

Gurioli L, Zanella E, Gioncada A, Sbrana A (2012) The historic magmatic-hydrothermal eruption of the Breccia di Commenda, Vulcano, Italy. Bull Volcanol 74:1235–1254

Keller J (1970) Die historischen eruptionen von Vulcano und Lipari. Z Deutsch Geol Ges 121:179–185

Keller J (1980) The island of Vulcano. Rend Soc Ital Miner Petrol 36:369–414

Lanza R, Zanella E (2003) Paleomagnetic secular variation at Vulcano (Aeolian Islands) during the last 135 kyr. Earth Planet Sci Lett 213:321–336

Lanza R, Meloni A, Tema E (2005) Historical measurements of the Earth's magnetic field compared with remanence directions from lava flows in Italy over the last four centuries, Phys. Earth Planet Inter 148:97–107

Macedonio G, Costa A, Folch A (2008) Ash fallout scenarios at Vesuvius: numerical simulations and implications for hazard assessment. J Volcanol Geotherm Res 178:3, 366-377

Manni M, Rosi M (2021) Origins of Vulcanello based on the re-examination of historical sources (Vulcano, Aeolian Islands). Ann Geophysics 65(5) in press.

Mercalli G, Silvestri O (1891) Le eruzioni dell'isola di Vulcano, incominciate il 3 Augusto 1888 e terminate il 22 Marzo 1880. Ann Uff Centr Meteorol Geodin 10(4):1–213

Neri A, Bevilacqua A, Esposti Ongaro T, Isaia R, Aspinall WP, Bisson M, Flandoli F, Baxter PJ, Bertagnini A, Iannuzzi E, Orsucci S, Pistolesi M, Rosi M, Vitale S (2015) Quantifying volcanic hazard at Campi Flegrei caldera (Italy) with uncertainty assessment: 2. Pyroclastic density current invasion maps. J Geophys Res: Solid Earth, 120(4), 2330-2349

Nicotra E, Giuffrida M, Viccaro M, Donato P, D'Oriano C, Paonita A, De Rosa R (2018) Timescales of pre-eruptive magmatic processes at Vulcano (Aeolian Islands, Italy) during the last 1000 years. Lithos 316:347–365

Pallister JS, Clynne MA, Wright HM, Van Eaton AR, Vallance JW, Sherrod DR, Kokelaar BP (2017) Field-trip guide to Mount St. Helens, Washington-An overview of the eruptive history and petrology, tephra deposits, 1980 pyroclastic density current deposits, and the crater. Scientific Investigations Report, (2017-5022-D)

Pavón-Carrasco FJ, Rodríguez-González J, Osete ML, Torta JM (2011) A Matlab tool for archaeomagnetic dating. J Archaeol Sci 38:408–419

Pavón-Carrasco FJ, Osete ML, Torta JM, De Santis A (2014) A geomagnetic fieldmodel for the Holocene based on archaeomagnetic and lava flow data. Earth Planet Sci Lett 388:98–109

Pavón- Carrasco FJ, Campuzano SA, Rivero- Montero M, Molina- Cardín A, Gómez- Paccard M, Osete ML (2021) SCHA.DIF.4k: 4,000 Years of Paleomagnetic Reconstruction for Europe and Its Application for Dating. J Geophys Res: Solid Earth 126(3):e2020JB021237

Pinton A, Giordano G, Speranza F, Þórðarson Þ (2018) Paleomagnetism of Holocene lava flows from the Reykjanes Peninsula and the Tungnaà lava sequence (Iceland): implications for flow correlation and ages. Bull Volcanol 80:10

Pistolesi M, Rosi M, Cioni R, Cashman KV, Rossotti A, Aguilera E (2011) Physical volcanology of the post–twelfth-century activity at Cotopaxi volcano, Ecuador: Behavior of an andesitic central volcano. Bulletin 123(5-6), 1193-1215

Pistolesi M, Rosi M, Malaguti AB, Lucchi F, Tranne CA, Speranza F, Albert PG, Smith V, Di Roberto A, Billotta E (2021) Chrono-stratigraphy of the youngest (last 1500 years) rhyolitic eruptions of Lipari (Aeolian Islands, Southern Italy) and implications for distal tephra correlations. J Volcanol Geotherm Res 420:107397

Ramsey CB (2009) Bayesian analysis of radiocarbon dates. Radiocarbon 51(1):337-360

Reimer PJ, Austin WE, Bard E, Bayliss A, Blackwell PG, Bronk Ramsey C, Butzin M, Cheng H, Lawrence Edwards R, Friedrich M, Grootes PM, Guilderson TP, Hajdas I, Heaton TJ, Hogg AG, Hughen KA, Kromer B, Manning SW, Muscheler R, Palmer JG, Pearson C, van der Plicht J, Reimer RW, Richards DA, Marian Scott E, Southan JR, Turney CSM, Wacker L, Adolphi F, Büntegen U, Capano M, Fahrni SM, Fogtmann-Schulz A, Friedrich R, Köhler P, Kudsk S, Miyake F, Olden J, Reinig F, Sakamoto M, Sookdeo A, Talamo S (2020) The IntCal20 Northern Hemisphere radiocarbon age calibration curve (0–55 cal kBP). Radiocarbon 62(4):725-757

Risica G, Speranza F, Giordano G, De Astis G, Lucchi F (2019) Palaeomagnetic dating of the Neostromboli succession. J Volcanol Geotherm Res 371:229–244

Romagnoli C, Casalbore D, Bosman A, Braga R, Chiocci FL (2013) Submarine structure of Vulcano volcano (Aeolian Islands) revealed by high-resolution bathymetry and seismo-acoustic data. Mar Geol 338:30–45

Rosi M, Di Traglia F, Pistolesi M, Ongaro TE, Vitturi MDM, Bonadonna C (2018) Dynamics of shallow hydrothermal eruptions: new insights from Vulcano's Breccia di Commenda eruption. Bull Volcanol 80(12):83

Ruch J, Vezzoli L, De Rosa R, Di Lorenzo R, Acocella V (2016) Magmatic control along a strike-slip volcanic arc: the central Aeolian arc (Italy). Tectonics 35:407–424

Scaillet B, Pichavant M, Cioni R (2008) Upward migration of Vesuvius magma chamber over the past 20,000 years. Nature, 455(7210), 216-219

Selva J, Bonadonna C, Branca S, De Astis G, Gambino S, Paonita A, Pistolesi M, Ricci T, Sulpizio R, Tibaldi A, Ricciardi A (2020) Multiple hazards and paths to eruptions: A review of the volcanic system of Volcano (Aeolian Islands, Italy). Earth-Science Reviews 103186

Soligo M, De Astis G, Delitala MC, La Volpe L, Taddeucci A, Tuccimei P (2000) Uranium-series disequilibria in the products from Vulcano Island (Sicily, Italy): isotopic chronology and magmatological implications. Acta Vulcanol 12:49–59

Speranza F, Branca S, Coltelli M, D'ajello Caracciolo F, Vigliotti L (2006) How accurate is "paleomagnetic dating"? New evidence from historical lavas from Mount Etna. J Geophys Res 111(B12)

Speranza F, Pompilio M, D'Ajello Caracciolo F, Sagnotti L (2008) Holocene Eruptive history of the Stromboli volcano: constraints paleomagnetic dating. J Geophys Res 113(B9).

Todman A (2012) Temporal and spatial variations in the geochemistry of recent (<2ka) volcanic rocks from Vulcano, Aeolian Islands, Italy. MPhil, Royal Holloway, University of London

Van der Voo R (1990) The reliability of paleomagnetic data. Tectonophysics184:1–9

Ventura G, Vilardo G, Milano G, Pino NA (1999) Relationships among crustal structure, volcanism and strike-slip tectonics in the Lipari-Vulcano volcanic complex (Aeolian Islands, Southern Tyrrhenian Sea, Italy). Phys Earth Planet Inter116:31–52

Voltaggio M, Branca M, Tuccimei P, Tecce F (1995) Leaching procedure used in dating young potassic volcanic rocks by the $^{226}Ra/^{230}Th$ method. Earth Planet Sci Lett136: 123–131

Yamamoto T (2017) Field guide of Izu-Oshima Volcano. Bulletin of the Geological Survey of Japan 68.4: 163-175

Zanella E (2006) Magnetic chronology in recent volcanic rocks: basic principles and case histories from Aeolian Islands. Acta Vulcanol 18:35–46

FIGURES AND TABLES

Figure 1: Geology of La Fossa cone and Vulcanello modified after De Astis et al. (2013), Di Traglia et al. (2013) and Fusillo et al. (2015). The location of the paleomagnetic sampling sites and the position of ^{14}C samples from this work are shown. DTM is derived from a 2-m resolution Lidar point cloud acquired in 2017 by Ministero dell'Ambiente for the entire island (MATTM; www.minambiente.it).

Figure 2: (a) One of the trenches dug on the southern side of La Fossa Cone, where the tephra sequence between PalD and Breccia di Commenda deposits and associated to effusive activity is exposed. (b) The white to gray ash and lapilli tephra associated to the emplacement of the Commenda lava. (c) The stratigraphic unconformity (S3) separating the final BdC varicolored ash from the onset of the Gran Cratere activity. (d) Locations of trenches and natural outcrops used for tephra correlation and shown in Figures 2 and 3. (e) Welded scoriae of the Punte Nere formation overlying older volcanic deposits at Levante harbor; Punte Nere Cape is on the left side

of the photo. DTM is derived from a 2-m resolution Lidar point cloud acquired in 2017 by Ministero dell'Ambiente for the entire island (MATTM; www.minambiente.it).

Figure 3: Trenches and outcrops (top) and relative stratigraphic reconstructions (bottom) of key sections at Vulcanello (a, b and c) and La Fossa (d). Locations are also shown in Figure 2d.

Figure 4: Representative outcrop pictures of some of the paleomagnetic sampling sites. (a) Overview of the Vulcanello Cones. (b) View of the Punte Nere lava flow. (c) Detail of the dike exposed on the cliff of the Cone I (Vulcanello peninsula). (d) Particular of Vulcanello Cone I (e) Overview of the Palizzi lava flow. (f) Particular of Punte Nere welded scoriae. (g) Overview of the Punta Roveto lava flow. (h) The Valle dei Mostri lava flow.

Figure 5: Representative orthogonal vector diagrams of typical alternating field demagnetization data, in situ coordinates. Open and solid dots represent projections on the vertical and horizontal planes, respectively. Demagnetization step values are in mT.

Figure 6: Equal-area projection (lower hemisphere) of site-mean paleomagnetic directions from La Fossa cone (a) and Vulcanello peninsula (b). The ellipses around the paleomagnetic directions are the projections of the relative α_{95} cones. All the paleomagnetic directions are listed in Table 3.

Figure 7: Paleomagnetic datings of La Fossa and Vulcanello according to the method and software by Pavón-Carrasco et al. (2011), and the paleo-secular variation (PSV) reference model by Pavón-Carrasco et al. (2014, 2021). In left-hand panel PSV curves for the declination and in the right-hand panel the inclination are shown as thick red lines (thin red lines for the associated errors, 95% confidence level), together with the probability density curves (in grey-shade below each PSV). Palaeomagnetic declination and inclination values are shown in the PSV graphs as blue straight

lines; the green dashed lines above and below are the 95% associated errors. The final combined probability density curves are shown in grey-shade (the 95% confidence level is shown as a green line).

Figure 8: Chronostratigraphic relationships between La Fossa Cone and Vulcanello activity during the last 1100 years. Age references: (1) Arrighi et al. (2006); (2) Frazzetta et al. (1983); (3) Pistolesi et al. (2021); (4) Keller (1970); this work (in bold). Tephra markers traceable at La Fossa and Vulcanello are also reported in bold and red. Stratigraphic unconformities in italic (S1, S2 and S3) are from Di Traglia et al. (2013).

Table 1: Synthesis of the geochronological constraints on eruption ages at La Fossa cone and Vulcanello peninsula during the last 6 ka.

Table 2: Results of radiocarbon age determinations and calendar age conversion. Sampling locations and sample stratigraphic heights are also indicated.

Table 3: Mean paleomagnetic directions from Vulcano island and paleomagnetic dating.

Figure 1

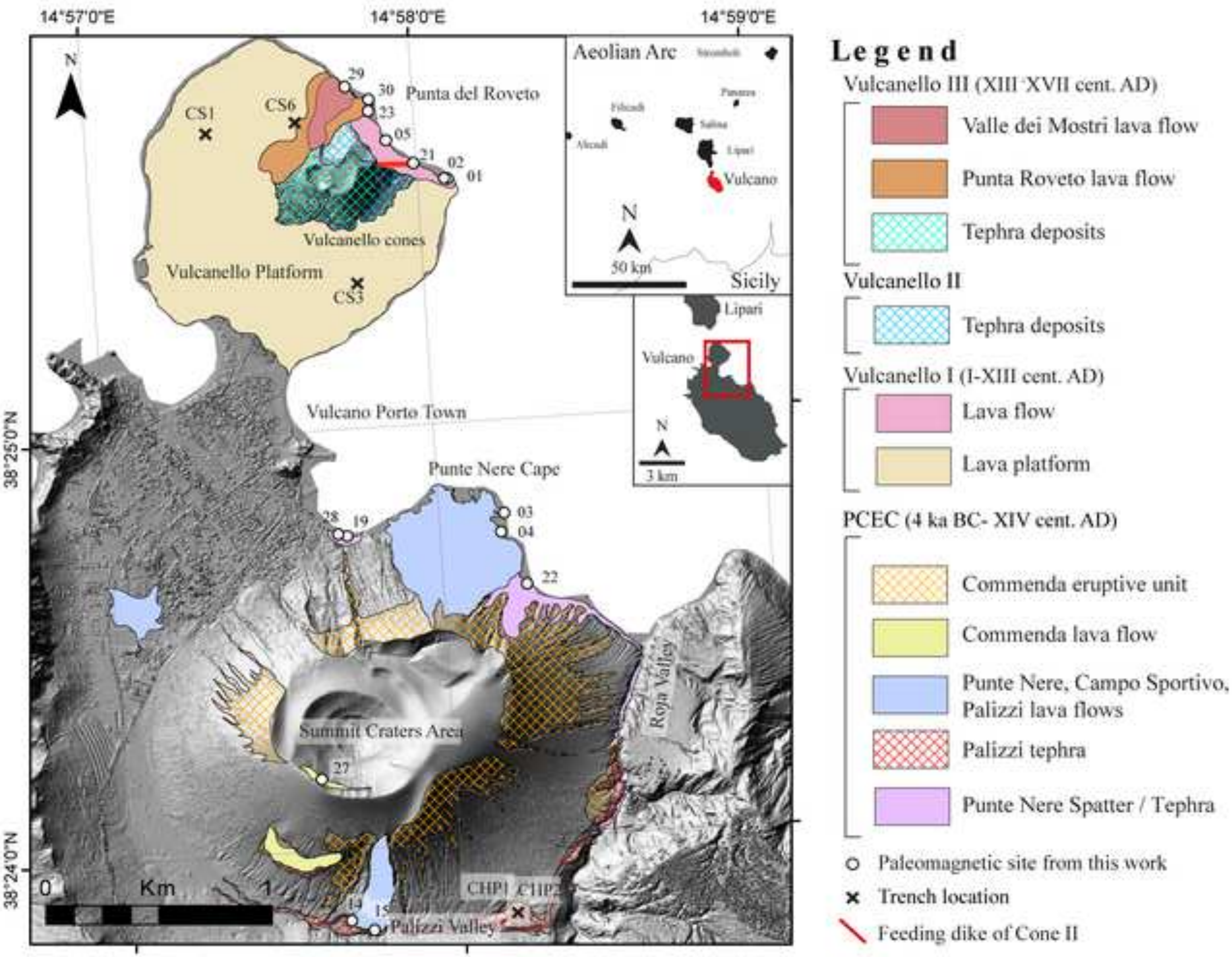
14°57'0"E
14°58'0"E
14°59'0"E
38°25'0"N
38°24'0"N
N
Punta del Roveto
CS1
CS6
CS3
29
30
23
05
21
02
01
Vulcanello cones
Vulcanello Platform
Vulcano Porto Town
Punte Nere Cape
28
19
03
04
22
Summit Craters Area
27
Roja Valley
CHP1
CHP2
14
15
Palizzi Valley
0
Km
1
Aeolian Arc
Filicudi
Alicudi
Salina
Panarea
Lipari
Vulcano
Sicily
50 km
Lipari
Vulcano
3 km
Legend
Vulcanello III (XIII-XVII cent. AD)
Valle dei Mostri lava flow
Punta Roveto lava flow
Tephra deposits
Vulcanello II
Tephra deposits
Vulcanello I (I-XIII cent. AD)
Lava flow
Lava platform
PCEC (4 ka BC- XIV cent. AD)
Commenda eruptive unit
Commenda lava flow
Punte Nere, Campo Sportivo, Palizzi lava flows
Palizzi tephra
Punte Nere Spatter / Tephra
Paleomagnetic site from this work
Trench location
Feeding dike of Cone II

Figure 2

Click here to access/download;Figure;Fig. 2.tif

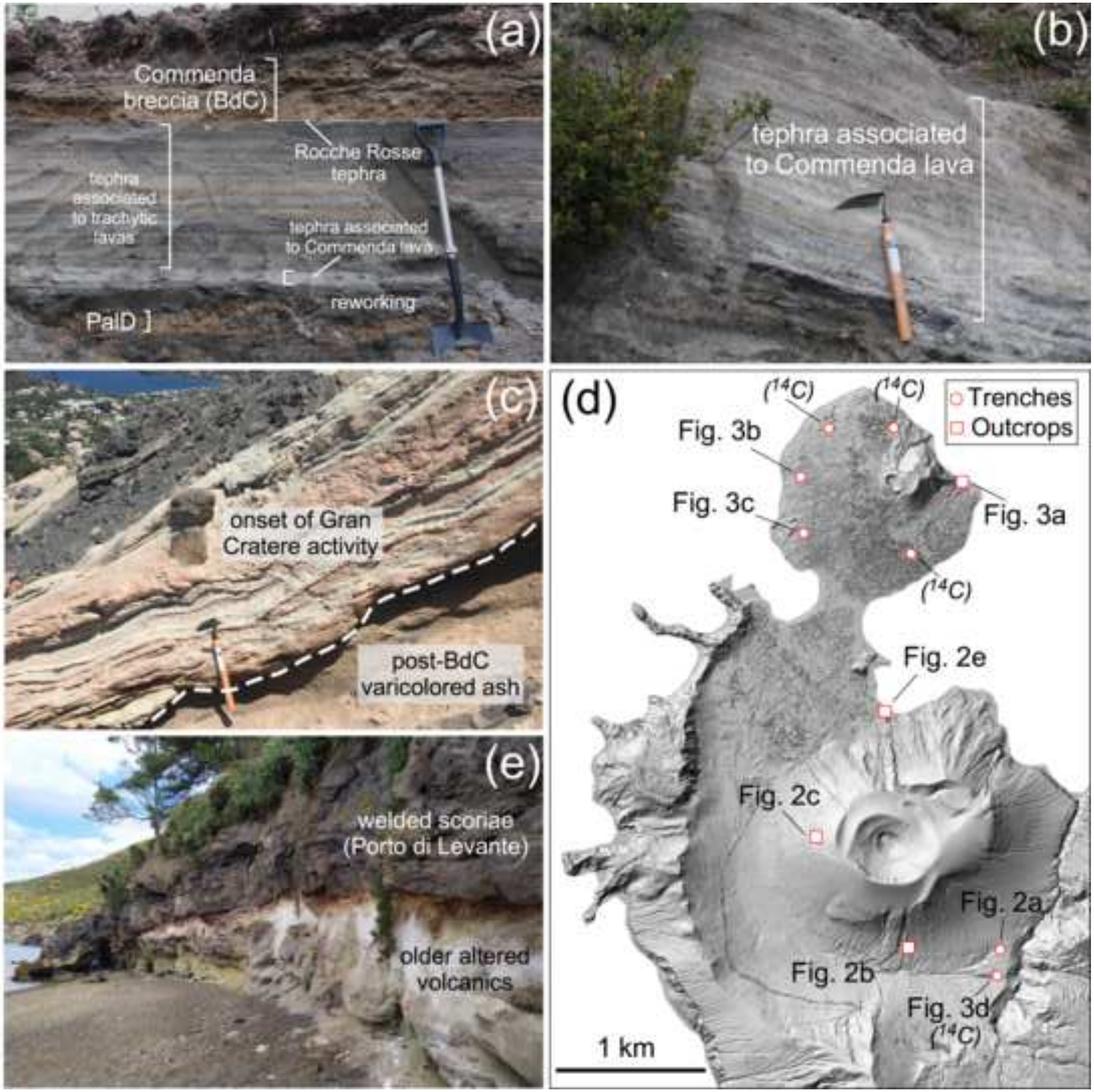

Figure 3

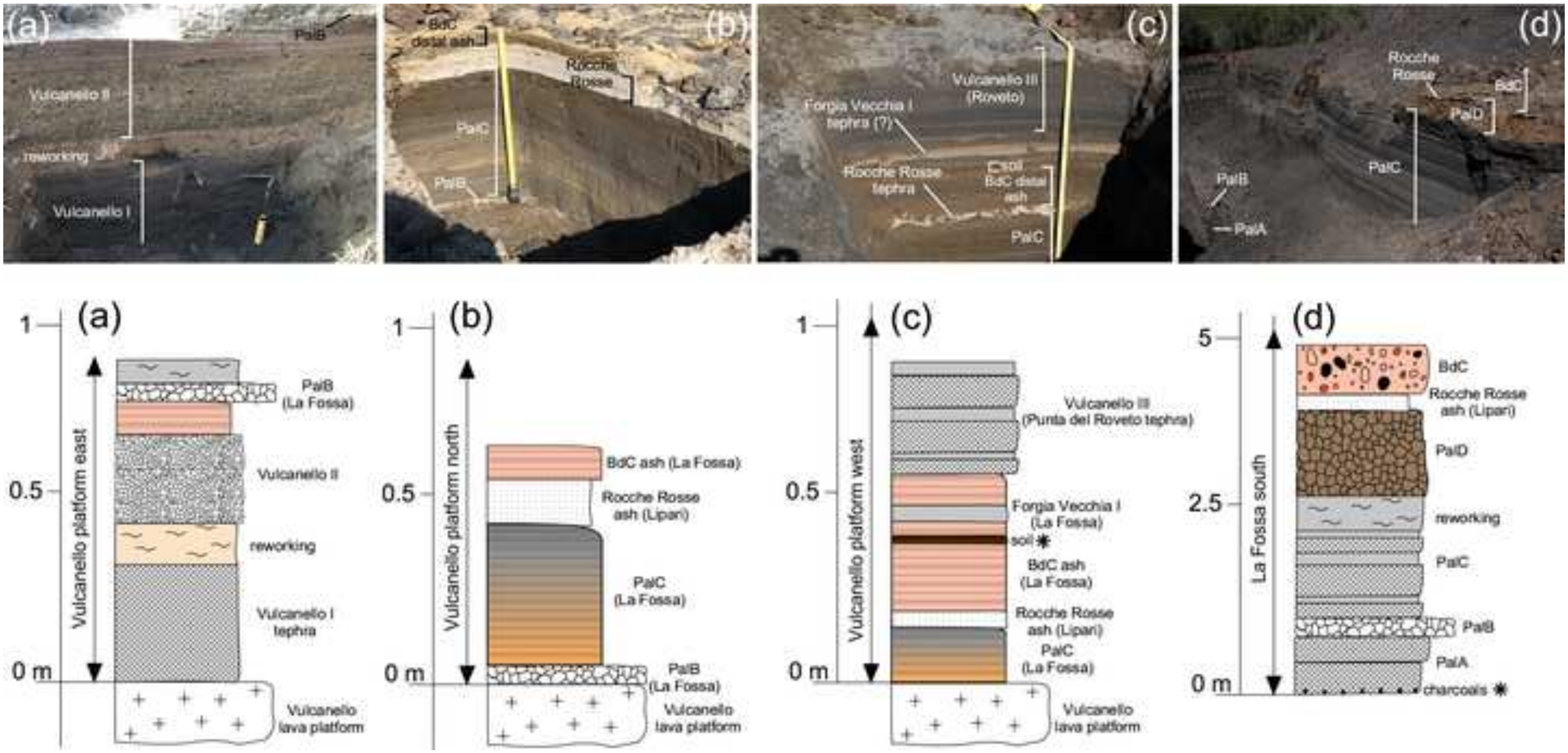
(a)
PalB
Vulcanello II
reworking
Vulcanello I
(b)
BdC distal ash
Rocche Rosse
PalC
PalB
(c)
Vulcanello III (Roveto)
Forgia Vecchia I tephra (?)
Rocche Rosse tephra
soil
BdC distal ash
PalC
(d)
Rocche Rosse
BdC
PalD
PalC
PalB
PalA
1
(a)
0.5
0 m
Vulcanello platform east
PalB (La Fossa)
Vulcanello II
reworking
Vulcanello I tephra
Vulcanello lava platform
1
(b)
0.5
0 m
Vulcanello platform north
BdC ash (La Fossa)
Rocche Rosse ash (Lipari)
PalC (La Fossa)
PalB (La Fossa)
Vulcanello lava platform
1
(c)
0.5
0 m
Vulcanello platform west
Vulcanello III (Punta del Roveto tephra)
Forgia Vecchia I (La Fossa)
soil
BdC ash (La Fossa)
Rocche Rosse ash (Lipari)
PalC (La Fossa)
Vulcanello lava platform
5
(d)
2.5
0 m
La Fossa south
BdC
Rocche Rosse ash (Lipari)
PalD
reworking
PalC
PalB
PalA
charcoals

Figure 4

Click here to access/download;Figure;Fig. 4.tif

Figure 5

Click here to access/download;Figure;Fig. 5.tif

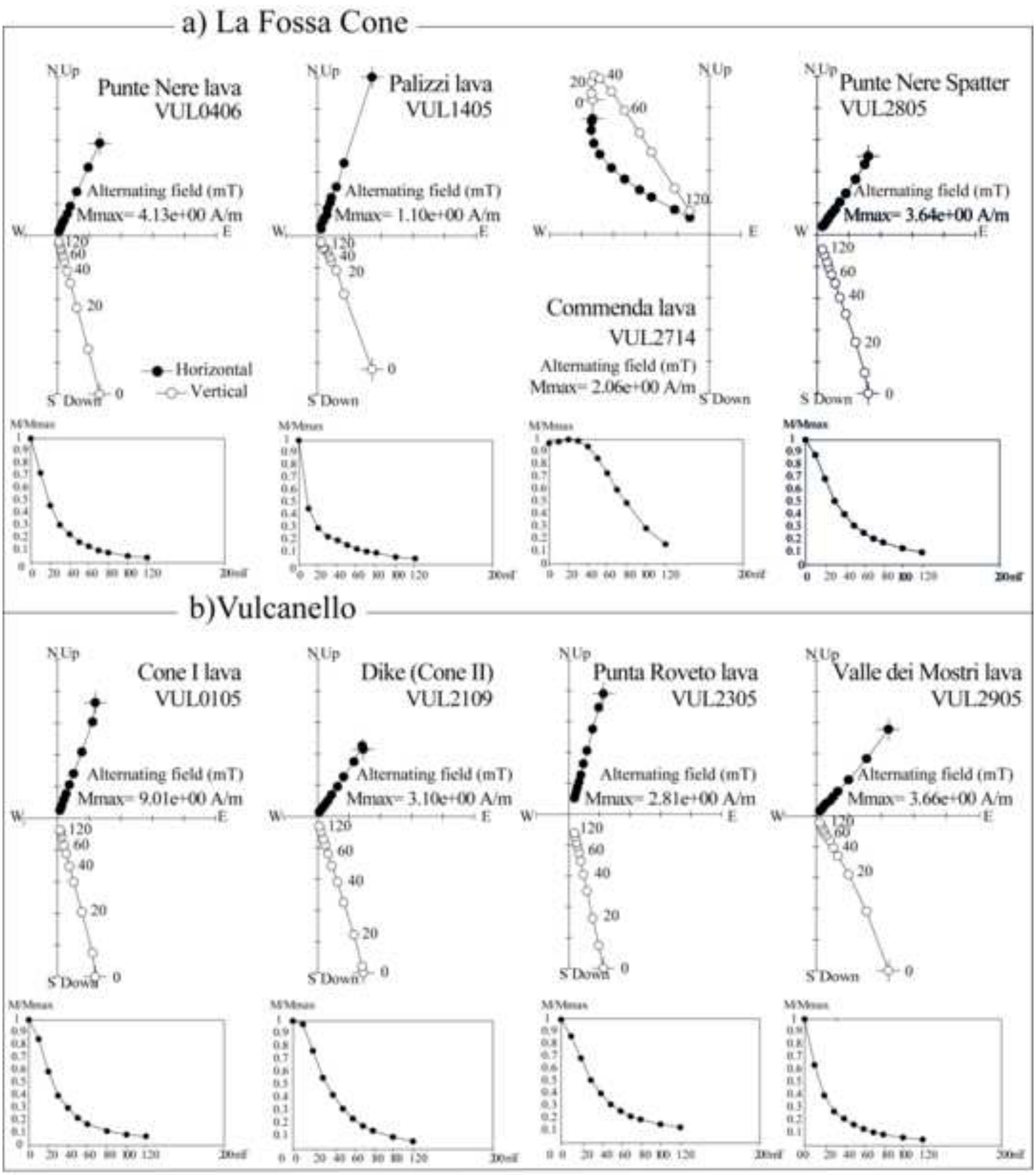

Figure 6

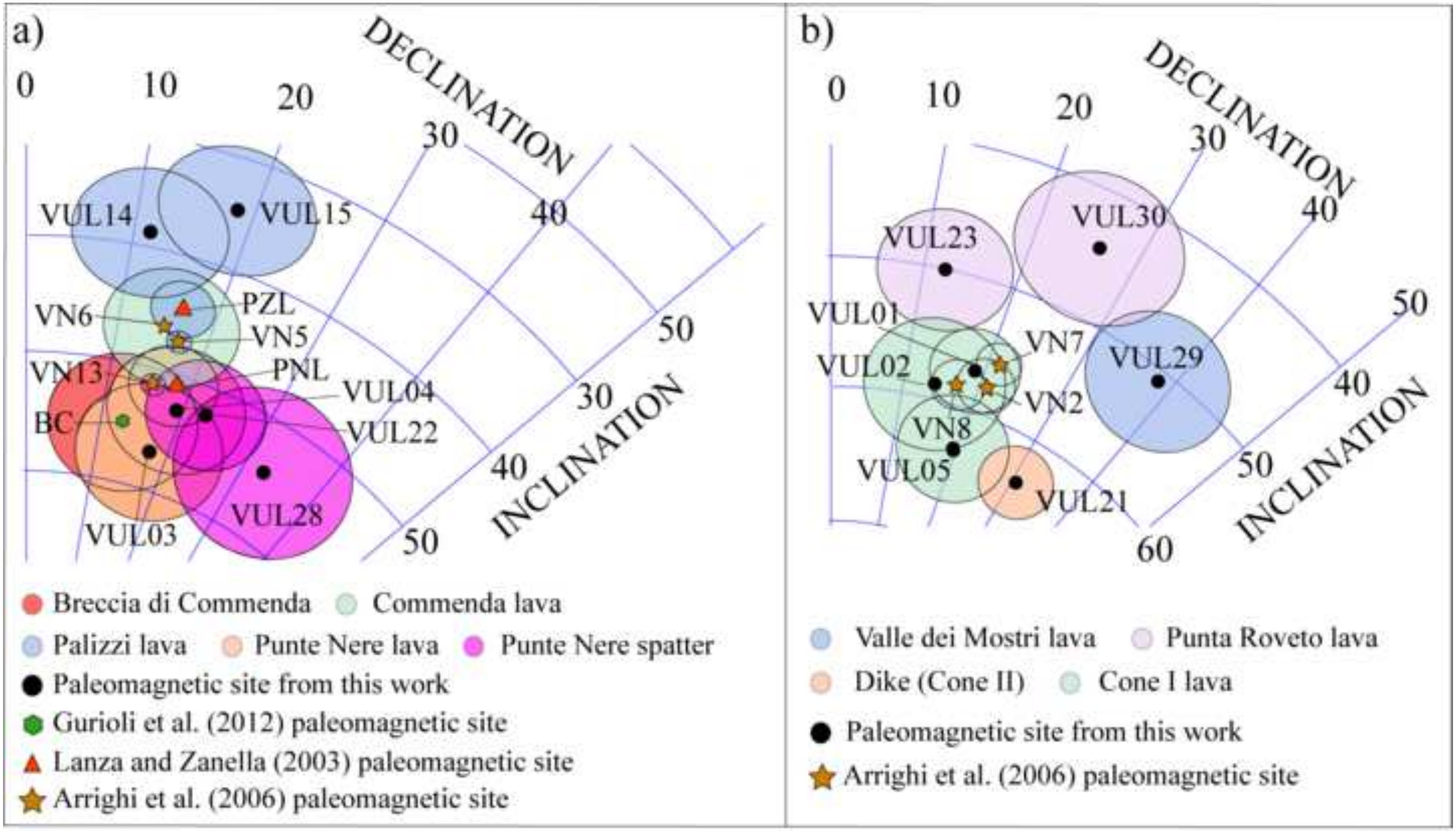
a)
DECLINATION
INCLINATION
0
10
20
30
40
50
VUL14
VUL15
VN6
PZL
VN5
VN13
PNL
VUL04
BC
VUL22
VUL28
VUL03
Breccia di Commenda
Commenda lava
Palizzi lava
Punte Nere lava
Punte Nere spatter
Paleomagnetic site from this work
Gurioli et al. (2012) paleomagnetic site
Lanza and Zanella (2003) paleomagnetic site
Arrighi et al. (2006) paleomagnetic site
b)
DECLINATION
INCLINATION
60
VUL23
VUL30
VUL01
VN7
VUL02
VUL29
VN2
VN8
VUL05
VUL21
Valle dei Mostri lava
Punta Roveto lava
Dike (Cone II)
Cone I lava
Paleomagnetic site from this work
Arrighi et al. (2006) paleomagnetic site

Figure 7

Click here to access/download;Figure;Fig. 7.tif

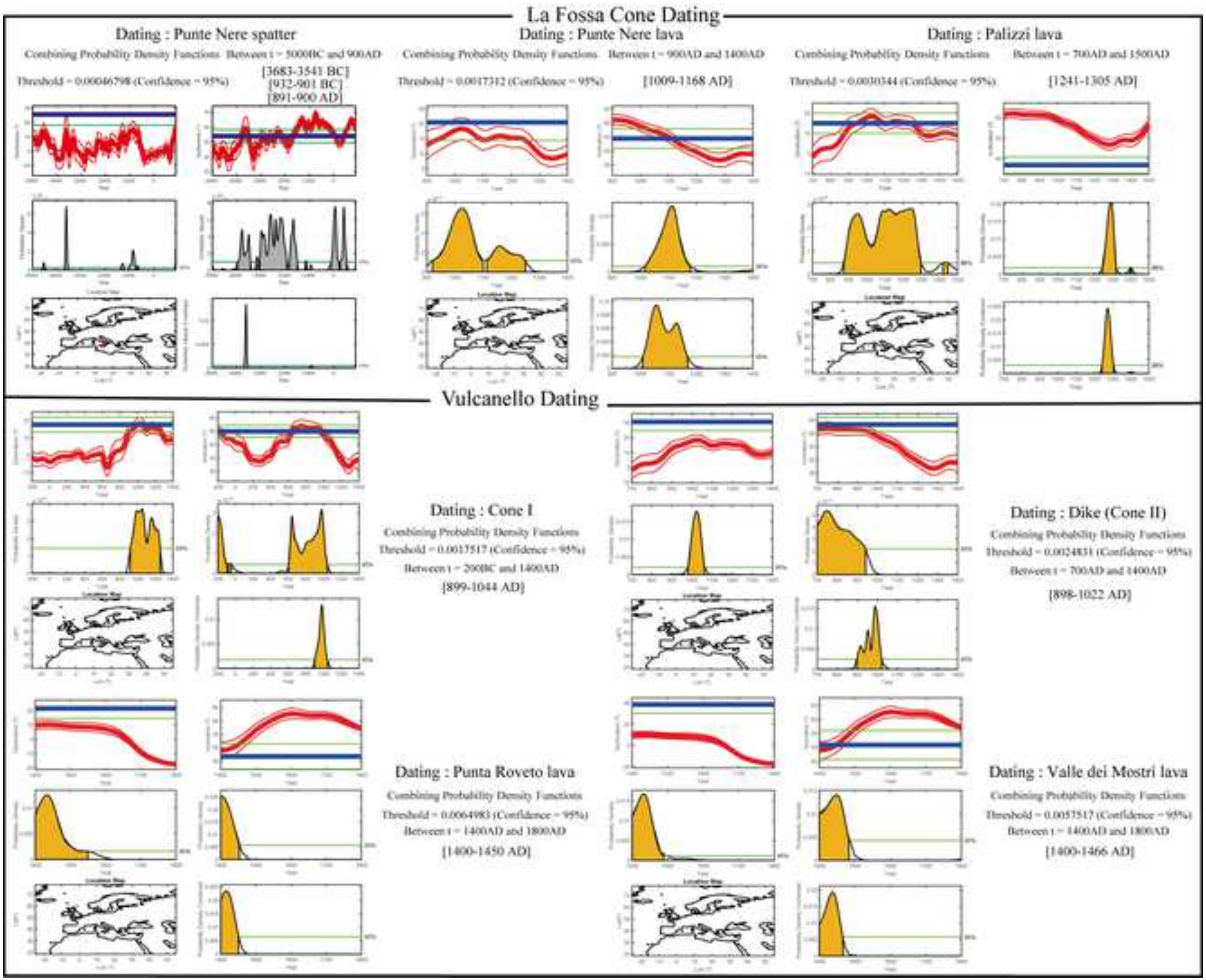

Figure 8

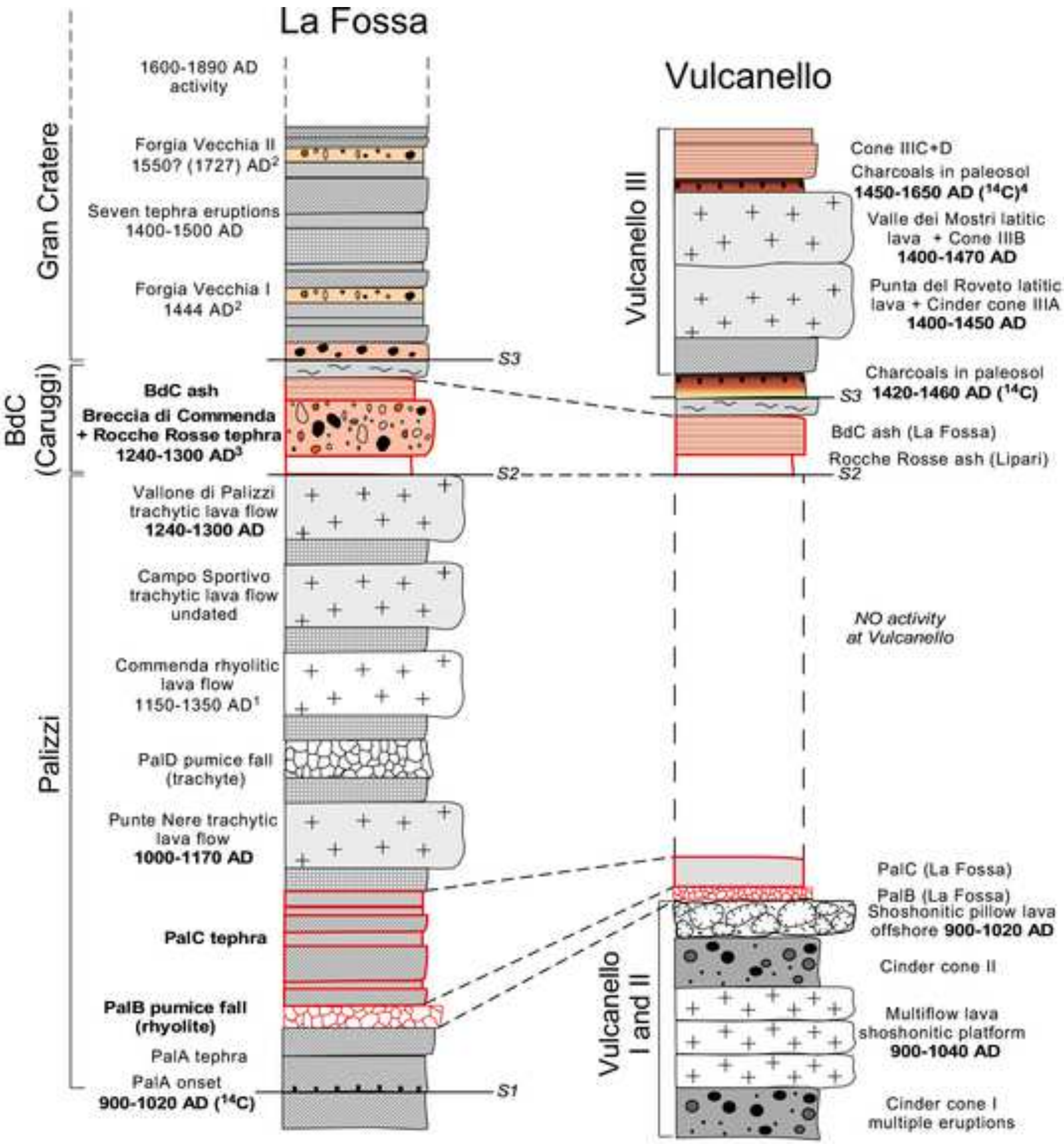

La Fossa
Vulcanello
Gran Cratere
1600-1890 AD activity
Forgia Vecchia II 1550? (1727) AD²
Seven tephra eruptions 1400-1500 AD
Forgia Vecchia I 1444 AD²
S3
BdC (Caruggi)
BdC ash
Breccia di Commenda + Rocche Rosse tephra 1240-1300 AD³
S2
Palizzi
Vallone di Palizzi trachytic lava flow 1240-1300 AD
Campo Sportivo trachytic lava flow undated
Commenda rhyolitic lava flow 1150-1350 AD¹
PalD pumice fall (trachyte)
Punte Nere trachytic lava flow 1000-1170 AD
PalC tephra
PalB pumice fall (rhyolite)
PalA tephra
PalA onset 900-1020 AD (¹⁴C)
S1
Vulcanello III
Cone IIIC+D
Charcoals in paleosol 1450-1650 AD (¹⁴C)⁴
Valle dei Mostri latitic lava + Cone IIIB 1400-1470 AD
Punta del Roveto latitic lava + Cinder cone IIIA 1400-1450 AD
Charcoals in paleosol 1420-1460 AD (¹⁴C)
BdC ash (La Fossa)
Rocche Rosse ash (Lipari)
NO activity at Vulcanello
PalC (La Fossa)
PalB (La Fossa)
Shoshonitic pillow lava offshore 900-1020 AD
Cinder cone II
Multiflow lava shoshonitic platform 900-1040 AD
Cinder cone I multiple eruptions
Vulcanello I and II

Table 1

	De Fiore (1922) historical records	Mercalli and Silvestri (1891) historical records	Keller (1970) ^{14}C dating	Frazzetta et al. (1984) K/Ar dating	Voltaggio et al. (1995) Ra^{266}/Th^{230} dating	Soligo et al. (2000) Ra^{266}/Th^{230} dating	Zanella (2006) Paleomag dating	Arrighi et al. (2006) Paleomag dating	Gurioli et al. (2012) Paleomag dating
Vulcanello III (paleosoil)			397±97 yr BP (1553±97 AD)						
Vulcanello Cone I								1050±70 AD 1080±50 AD 1000±60 AD	
Vulcanello I Platform	183/126/91 BC (early emersion)	183/126/91 BC			1.9±0.2 ka BP (50 AD ±0.2 ka)			1180±30 AD 1189±70 AD 1230±30 AD 1100±60 AD	
Breccia di Commenda									918-1302 AD 1399-1604 AD
Commenda lava flow								1250±100 AD	
Palizzi lava flow				1.6±1.0 ka BP (350 AD ±1.0 ka)	1.5+0.2 ka BP (450 AD+0.2 ka)		1200-1413 AD	1230±20 AD	
Palizzi Pyroclastic products				2.2±1.3 ka BP (250 BC ±1.3 ka)					
Punte Nere lava flow				5.5±1.3 ka BP (3550 BC ±1.3 ka)		3.8 (+0.9/-0.8) ka BP (1850 BC +0.9/-0.8 ka)		1170 ± 20 AD or prehistoric (?)	
Punte Nere Pyroclastic products						5.3 (+2.2/-1.1) ka BP (3350 BC +2.2/-1.1 ka)			

Table 2

Sample	Type of sample	Method	Location (site)	Stratigraphic height	$d^{13}C$	Uncalibrated Date	Calibrated Date (BP)	Calibrated Date (AD)
CS1	Charred material	AMS	NW Vulcanello (hand-dug pit)	Soil below Punta del Roveto tephra	-22.9	448 ± 25	506 ± 26	1419 - 1470
CS3	Charred material	AMS	SE Vulcanello (machine excavated trench)	Soil below Punta del Roveto tephra	-26.39	461± 26	514 ± 22	1414 - 1458
CS6	Charred material	AMS	N Vulcanello (hand-dug pit)	Embedded in Breccia di Commenda ash	-26.19	717 ± 22	671 ± 19	1260 - 1298
CHP1	Charred material	AMS	S La Fossa (machine excavated trench)	Below PalA ash	-23.06	1084 ± 24	995 ± 60	895 - 1015
CHP2	Charred material	AMS	S La Fossa (machine excavated trench)	Below PalA ash	-23.61	1086 ± 25	995 ± 61	896 - 1015

Table 3

Volcanic Unit	Code	n/N	D, deg	I, deg	k	α_{95}, deg	Paleomagnetic dating (yr BC-AD)	Reference
Punte Nere lava	PNL	1/12	17.9	51	164	3.4		1
Punte Nere Spatter	VN13	15/15	15.5	51.4	1,543	0.92	1170±20 AD or prehistoric	2
Punte Nere lava	VUL03	9/11	17.5	56.9	82.1	5.7		4
Punte Nere lava	VUL04	11/11	22.8	52.4	98.2	4.6		4
Punte Nere spatter	VUL19*	10/10	21.4	45.5	21.9	10.6		4
Punte Nere spatter	VUL22	8/10	19.2	52.9	110	5.3		4
Punte Nere spatter	VUL28	7/10	32.7	54.4	74.4	7		4
	Sample mean (VUL03+VUL04)	20/22	20.5	54.5	85.8	3.5	1009-1168 AD	4
	Sample mean (VUL22+VUL28)	15/20	25.4	53.8	77.1	4.4	3683-3541 BC 932-901 BC 891-900 AD	4
Palizzi lava	PZL	1/8	16.4	44.5	514	2.4		1
Palizzi lava	VN5	13/16	17	47.3	1,693	0.94	1230±20 AD	2
Palizzi lava	VUL14	10/10	11.5	38.6	71.6	5.7		4
Palizzi lava	VUL15	9/10	18.5	34.7	81.8	5.7		4
	Sample mean (VUL14+VUL15)	19/20	14.9	36.8	70.1	4	1241-1305 AD	4
Commenda Lava	VN6	15/16	15.8	46.3	51	5.1	1250±100 AD	2
Commenda Lava	VUL27*	17/17	29.2	32.9	1.4	50.3		4
Breccia di Commenda	BC	23/38	12.9	55.1		5.8	918-1302 AD 1399-1604 AD	3
Cone I lava	VN2	11/12	20.8	57.8	410	2.06	1050±70 AD	2
Cone I lava	VN7	10/10	21.4	55.9	767	1.6	1080±50 AD	2
Cone I lava	VN8	8/8	17.3	58.4	678	1.9	1000±60 AD	2
Cone I lava	VUL01	8/10	18.8	57	292.9	3.2		4
Cone I lava	VUL02	9/12	14.2	58.8	106.5	5		4
Cone I lava	VUL05	11/15	19.6	63.2	133.4	4		4
	Sample mean (VUL01+VUL02+VUL05)	28/37	17.6	60	128.9	2.4	899-1044 AD	4
Dike (Cone II)	VUL 21	15/15	30.7	63.4	195.8	2.7	898-1022 AD	4
Punta Roveto lava	VUL23	5/11	12.3	50.1	261.7	4.7		4
Punta Roveto lava	VUL30	9/10	26.2	44.5	77	5.9		4
	Sample mean (VUL23+VUL30)	14/21	21.5	46.7	73.3	4.7	1400-1450 AD	4
Valle dei Mostri lava	VUL29	10/12	38.4	50.9	87.1	5.2	1400-1466 AD	4

n/N is the number of ChRM directions used to calculate the site-mean direction /total number of cores drilled at a site, or number of ChRM directions used to calculate the volcanic unit-mean direction/total number of cores drilled in the volcanic unit. D is paleomagnetic declination and I is inclination, k and α_{95} are statistical parameters after Fisher (1953). Paleomagnetic dating was carried out using the Matlab tool of Pavón-Carrasco et al. (2011). The unit-mean paleomagnetic directions were compared with the recent SCHA.DIF.4K PSV regional model by Pavón-Carrasco et al. (2021), and -just for the likely older Punte Nere Spatter- with the SHA.DIF.14K PSV global model (Pavón-Carrasco et al. 2014). * discarded sites with scattered ChRMs. Paleomagnetic directions (1) is from Lanza and Zanella (2003); (2) is from Arrighi et al. (2006); (3) is from Gurioli et al. (2012); (4) is from this work. n/N Lanza and Zanella (2003) is the number of sites/ number of specimens. n/N for Arrighi et al. (2006) is the number of samples selected for calculation of the magnetic directions.